Biosci. Biotechnol. Biochem., **69** (3), 544–552, 2005

Highly Active Mutants of Carbonyl Reductase S1 with Inverted Coenzyme Specificity and Production of Optically Active Alcohols

Souichi MORIKAWA,[1,†] Takahisa NAKAI,[1] Yoshihiko YASOHARA,[2] Hirokazu NANBA,[2] Noriyuki KIZAKI,[2] and Junzo HASEGAWA[3]

[1]*Life Science Research Laboratories, Kaneka Corporation, 1-8 Miyamae-machi, Takasago-cho, Takasago, Hyogo 676-8688, Japan*
[2]*Fine Chemicals Research Laboratories, Kaneka Corporation, 1-8 Miyamae-machi, Takasago-cho, Takasago, Hyogo 676-8688, Japan*
[3]*Life Science RD Center, Kaneka Corporation, 1-8 Miyamae-machi, Takasago-cho, Takasago, Hyogo 676-8688, Japan*

Received October 5, 2004; Accepted November 30, 2004

A wild type NADPH-dependent carbonyl reductase from *Candida magnoliae* (reductase S1) has been found not to utilize NADH as a coenzyme. A mutation to exchange the coenzyme specificity in reductase S1 has been designed by computer-aided methods, including three-dimensional structure modeling and *in silico* screening of enzyme mutants. Site-directed mutagenesis has been used to introduce systematic substitutions of seven or eight amino acid residues onto the adenosine-binding pocket of the enzyme according to rational computational design. The resulting S1 mutants show NADH-dependency and have lost their ability to utilize NADPH as a coenzyme, but retain those catalytic activities. Kinetic parameter V_{max} and K_m values of those mutants for NADH are 1/3- to 1/10-fold those of the wild type enzyme for NADPH. As a model system for industrial production of optically active alcohols, the S1 mutants can be applied to an asymmetric reduction of ketones, cooperating with a coenzyme-regeneration system that uses an NAD-dependent formate dehydrogenase.

Key words: carbonyl reductase; *Candida magnoliae*; coenzyme specificity; protein engineering

A reductase S1 (S1) is the carbonyl reductase isolated from *Candida magnoliae* AKU4643. It is applied to an asymmetric reduction of ethyl 4-chloro-3-oxobutanoate (COBE) to optically pure ethyl (*S*)-4-chloro-3-hydroxybutanoate ((*S*)-CHBE).[1,2] The wild type S1 is a member of the short-chain dehydrogenase and reductase (SDR) family;[3] it shows strict NADPH-dependency and cannot use NADH as a coenzyme. It has been applied to a good production system for optically active alcohols with a coenzyme-regenerating system containing glucose dehydrogenase (GDH) and glucose to recycle NADP+ to NADPH (Scheme 1).[4] Though GDH can regenerate both NADH and NADPH, this enzyme produces the equivalent of gluconic acid as a by-product, and occasionally it causes side-effects to the main reaction, resulting in the formation of an unfavorable optical isomer. On the other hand, formate dehydrogenase (FDH) is also useful as a regenerating enzyme for a coenzyme, but FDH interacts only with NADH.[5] Therefore, FDH is not able to couple with an NADPH-dependent carbonyl reductase such as S1. But, there are several advantages to employing FDH in an enzymatic reduction system. NADH is less expensive than NADPH, and the only resulting by-product from recycling NAD+ to NADH is carbon dioxide, FDH being inert to the substrate of the main reaction.[6] Hence we therefore attempted to modify the coenzyme dependency in S1 from NADPH-specific to NADH. We report herein the rational computational design of S1 mutants and the properties of the resulting mutants, and also show the synthesis of an optically active alcohol with the NADH-dependent S1 mutant utilizing the NADH regeneration system with FDH.

Several successful mutations and redesigns to exchange the coenzyme specificity of dehydrogenase or reductase using nicotinamide coenzyme have been reported, including glutathione reductase and dihydrolipoamide dehydrogenase (of the flavoprotein disulphide oxidoreductase family),[7,8] isocitrate dyhydrogenase and isopropylmalate dehydrogenase (of the decarboxylating dehydrogenase family),[9] lactate dehydrogenase,[10] leu-

† To whom correspondence should be addressed. Fax: +81-794-45-2459; E-mail: Souichi.Morikawa@kn.kaneka.co.jp

Abbreviations: 1D, one-dimensional; 3D, three-dimensional; (*S*)-CHBE, ethyl (*S*)-4-chloro-3-hydroxybutanoate; COBE, ethyl 4-chloro-3-oxobutanoate; CR, carbonyl reductase; DEE, dead-end elimination; FDH, formate dehydrogenase; GDH, glucose dehydrogenase; S1 (or reductase S1), NADPH-dependent carbonyl reductase from *Candida magnoliae*; S1Mx, S1M1, S1M2, *etc.*, mutant(s) of reductase S1; SDR, short-chain dehydrogenase and reductase

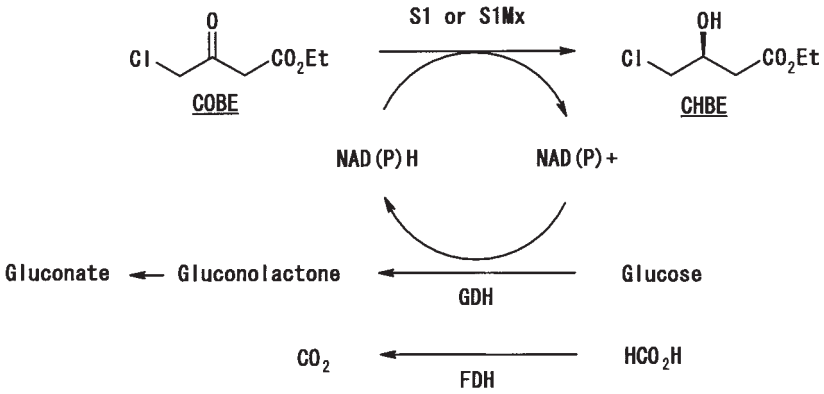

Scheme 1. Asymmetric Reduction of Ketone (COBE).

cine dehydrogenase,[11] and mouse lung carbonyl reductase (of the SDR family).[12] These results were obtained using empirical design methods derived from detailed analysis of amino acid sequences (one-dimensional (1D) structure) and/or atomic coordinates, as determined by X-ray analysis (three-dimensional (3D) structure). Considering the results of these empirical design methods, we have introduced a rational design method on the basis of the 3D structures of proteins and ligands (see methods section) to redesign the coenzyme specificity of the S1 mutant.

Materials and Methods

Summary of rational design. In the catalytic reaction with an enzyme, the ΔG_{bind} value of the enzyme and the substrate (or the coenzyme) molecule is generally equivalent to the Michaelis–Menten kinetic parameter K_{m} value of the enzyme for the substrate, according to the thermodynamic equation (1) in a simple enzymatic reaction process (2).

$$\Delta G_{\text{bind}} = RT \ln K_{\text{m}} \tag{1}$$

Here, ΔG_{bind} is the change in free energy in the process of binding the enzyme and substrate (or cofactor), K_{m} is the equilibrium constant (dissociation constant) of these molecules, and R and T are the gas constant and the temperature respectively.

$$\mathbf{E} + \mathbf{S} \overset{K_{\text{m}}}{\rightleftarrows} \mathbf{ES} \overset{k_{\text{cat}}}{\rightarrow} \mathbf{E} + \mathbf{P} \tag{2}$$

Here, **E**, **S**, and **P** are the enzyme, substrate, and product molecule respectively, the substrate and product molecules possibly being coenzymes or cofactors. The Michaelis–Menten kinetic parameters K_{m} and k_{cat} are the equilibrium constant (the dissociation constant) of **E** and **S**, and the velocity constant, respectively. The binding affinity of the enzyme mutants for the coenzyme can then be evaluated by comparing the difference ($\Delta\Delta G_{\text{bind}}$) of each of the ΔG_{bind} values between the mutants ($\Delta G_{\text{bind-mutant}}$) and the wild type (template) protein ($\Delta G_{\text{bind-wild-type}}$) (eq. 3).

$$\Delta\Delta G_{\text{bind}} = \Delta G_{\text{bind-mutant}} - \Delta G_{\text{bind-wild-type}} \tag{3}$$

Meanwhile, the thermostability of the enzyme should be considered in order to design the mutants available for practical use. It was assumed in this study that the thermostability of the protein can be evaluated by comparing the difference in the free energy change ΔG between the energy G_{N} of the properly folded native state (N state) and the energy G_{D} of the unfolded denatured state (D state) (eq. 4).

$$\Delta G = G_{\text{N}} - G_{\text{D}} \tag{4}$$

The ΔG is, in general, a free-energy change in the molecular system in the folding process of the protein. To compare the thermostability between a mutant and its template protein, the template usually being a wild type protein, it is necessary to compare the difference in the energy $\Delta\Delta G$ between the folding energies, ΔG_{mutant} and $\Delta G_{\text{wild-type}}$, of the mutant and wild type proteins respectively (eq. 5).

$$\Delta\Delta G = \Delta G_{\text{mutant}} - \Delta G_{\text{wild-type}} \tag{5}$$

The design method for the S1 mutants in this study involved *in silico* screening methods,[13] and was composed entirely of semi-automatic computational processes for (1) generation of mutant protein sequences from a template (wild type) protein sequence according to the input condition, (2) modeling of three-dimensional structures (*i.e.*, atomic coordinates of side-chains of amino acid residues) of those generated mutants with a dead-end elimination (DEE) algorithm,[14] and (3) evaluation of free-energy differences ($\Delta\Delta G_{\text{bind}}$) in the ligand-binding (here, coenzyme-binding) processes and evaluation of free-energy differences ($\Delta\Delta G$) in the folding processes between those mutants, by calculating roughly the AMBER molecular mechanics potential energy,[15] including the solvation energy term[16] *in vacuo*, and the change in the conformational entropy terms[17,18] by fixation of the main-chain and side-chains in the folding process.

Computer programs. The search for related SDR sequences and the multiple-alignment were performed by the BLAST program[19] and the Clustal-X program[20] respectively. The molecular graphics program Swiss

PDB Viewer[21] was used in the homology modeling of S1. Computational screenings were performed with the Shrike program.[13] The conditions of these calculations are included in the results section below.

Site-directed mutagenesis and expression. Substitutions for DNA sequences to produce the S1 mutants were introduced into plasmid pNTS1, which carries the S1 gene from *Candida magnoliae* inserted into pUCNT.[2,4] The recombinant plasmids of containing mutated cDNAs used in this study were constructed as follows: 167bp oligonucleotide fragments having the sequences of designed mutants (abbreviated as S1Mx, S1M1 to S1M8) were synthesized and inserted into the 3.2-kb DNA fragment, which was prepared by the digestion of pNTS1 with *Eco*O109I. The mutated plasmids pNTS1Mx were introduced into *E. coli* HB101. *E. coli* HB101 carrying pNTS1Mx (pNTS1M1 to pNTS1M8) was inoculated into a test tube containing 2 ml of 2xYT medium[4] supplemented with 50 μg/ml ampicillin, followed by incubation at 37 °C for 15 h. Cells were harvested from 1.5 ml of culture broth by centrifugation following suspension in 1.5 ml of 100 mM potassium phosphate buffer (pH 6.5), and then disrupted by ultrasonication. The cell debris was removed by centrifugation. The supernatant was recovered as cell-free extract for the enzyme assay. The S1M1 and S1M4 mutants were purified by procedure of Wada *et al.*,[1] which involves ammonium sulfate precipitation, DEAE-Sepharose column chromatography, and Phenyl-Sepharose column chromatography, to homogeneity on SDS polyacrylamide gel electrophoresis.

Enzyme assay and kinetic analysis. S1 and the S1Mx mutants were assayed spectrophotometrically. The standard reaction mixture, which consisted of 100 mM potassium phosphate buffer (pH 6.5), 0.167 mM NAD(P)H, 1 mM ethyl 4-chloroacetoacetate (COBE), and enzyme solution in a total volume of 3.0 ml, was monitored for a decrease in absorbance at 340 nm. One unit of enzyme activity was defined as the amount of enzyme catalyzing the oxidation of 1 μmol of NAD(P)H per min at 30 °C. Protein was measured with a protein assay kit from Bio-Rad, using bovine serum albumin as the standard. The kinetic constants, K_m and V_{max}, in the COBE reduction were calculated from double-reciprocal Lineweaver–Burk plots with a fixed saturated concentration of substrate or coenzyme. The thermostability of S1 and the mutants was measured with the residual catalytic activity in the COBE reduction after heat treatment of the enzyme solution (pH 7.0, potassium phosphate buffer) at 30, 35, 40, 45, 50, 55, and 60 °C for 30 min each.

Reduction of COBE with S1M4 and formate dehydrogenase (FDH) in a two-phase system. The aqueous solution of the reaction mixture consisted of 0.82 ml of the cell-free extract of S1M4 (340 U), 3.0 ml of the cell-free extract of haloketone-resistant FDH[22] (780 U), 6.3 ml of 5 M formic acid, 1.0 g of sodium formate, and 25 mg NAD+ in a total volume of 30 ml. To the aqueous solution, 30 ml of butyl acetate and 6.0 g of COBE were added, and the mixture was stirred at 30 °C. The pH of the mixture was adjusted to 6.5 with 5 M formic acid. CHBE concentrations were monitored by gas chromatography. The optical purity of CHBE was analyzed by HPLC, as described previously.[23]

Results

Multiple alignments of S1 and related SDRs

Amino acid sequences similar to the S1 sequence were obtained by the BLAST program applied to the nonredundant protein sequence database from NCBI. These sequences described or reported as having NADPH/NADH dependency were then selected. The resulting sequences were multiply aligned by the Clustal-X program, and those with known 3D structures were manually realigned by superimposition of their 3D structures on the molecular graphics program Swiss PDB Viewer. The result of multiple alignments of S1 and the related SDRs is shown in Fig. 1. The regions bound to the adenosine ribose moiety of the coenzyme (from Pro-14 to Gly-81 in S1) are shown in Fig. 1.

Homology modeling of the 3D structure of S1

A 3D structure model of S1 was prepared for the subsequent *in silico* screening. The 3D structures of 1YBV at the 14–215 residue positions and 1FMC at the 197–249 positions from the Protein Data Bank (PDB) were used as the template 3D stuructures to model S1. These corresponded to the 18–227 and 228–279 positions of S1 respectively. Several insertions, deletions, and substitutions of amino acid residues were performed with the program Swiss PDB Viewer. Neither insertions nor deletions were entered in secondary structures such as α-helices and β-sheets based on the conformational information. The preferable rotamers (sets of conformations) in the side-chains were evaluated by the DEE algorithm method for two enzyme–coenzyme complexes with NADPH and NADH respectively. Strains were then removed based on energy minimization calculations *in vacuo* with atomic restraints for the main-chain and nicotinamide heavy atoms. The resulting S1 model is shown in Fig. 2.

Screening of S1 mutants in silico

Several sets of computational screenings were performed with the Shrike program to search for reductase mutants having lower coenzyme affinity to NADPH, higher coenzyme affinity to NADH, and sufficient thermostability. The amino acid residue positions to mutate were selected from neighbors of adenosine 2′-phosphate ester (in NADPH) or adenosine 2′-OH (in NADH) of the coenzyme, according to an analysis of that modeled S1 structure. Here, the conserved motif

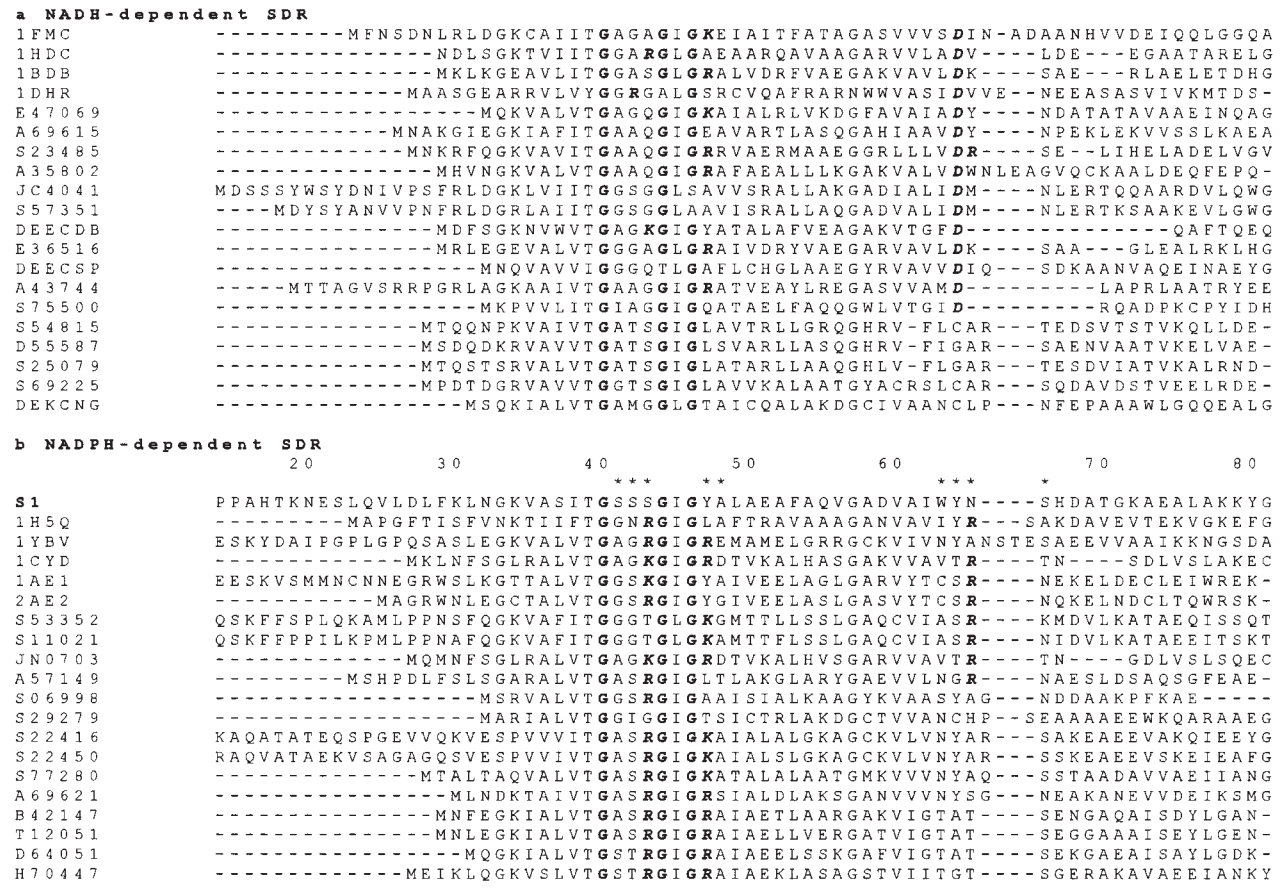

Fig. 1. Multiple Alignment of the Short-Chain Dehydrogenase/Reductase (SDR) Family.

The regions that bound to the adenosine ribose moiety of the coenzyme are shown in (a) NAD-dependent SDRs and (b) NADP-dependent SDRs. The residue position number is shown for S1 reductase. The mutated positions in this study are marked with asterisks (*). The conserved residues GXXXGXG are shown as bold characters. The residues Arg, Lys, and Asp that bound to 2′,3′-diol of NADH or to 2′-phosphate of NADPH are shown as bold and italic characters.

residues were excluded, and the residues finally selected to mutate were Ser-41, Ser-42, Ser-43, Tyr-47, Trp-63, Tyr-64, Asn-65, and Ser-66 of S1. These residues are positioned far from the binding pocket of the substrate compound and the reaction center of S1 in 3D space. As such, mutations of these residues should not influence the substrate specificity or the catalytic activity of the enzyme.

First, single-point mutations to the residues were calculated so as to limit residue types in the subsequent multiple-point mutation calculation. The residue types to be mutated to all included 20 natural amino acids in each position. The results of calculating the binding energy to the coenzyme and the thermostability of S1 mutants, which were mutated at residue Tyr-64, are shown in Table 1. It was assumed that mutation from Tyr-64 to Ala, Asn, or Asp would confer NADH-dependency to those S1 reductase mutants. These mutations were therefore selected and used in the following multiple-point mutation. The calculated mutation from Tyr-64 to Cys or Met also showed NADH-dependency, but the side-chains of these residues have weak reactivity and lesser robustness to halogeno-compounds such as COBE and CHBE, and these mutations were therefore not selected. The mutation from Tyr-64 to Leu or Val showed NADH-dependency, but the calculated thermostability of these holo-form (NADH complex) mutants was less than that of the wild type reductase, and these mutations were therefore not selected. Energy-decomposition analysis of the calculated mutants produced the following results: mutation from Tyr-64 to Asn, Asp, and Cys caused better electrostatic interaction between the enzyme and the coenzyme, and mutation to Ala, Met, Leu, and Val caused better van der Waals interactions within the enzyme itself (better packing of its hydrophobic core). On the other hand, the calculated results for the mutations to Tyr-64 showed worse NADPH-dependency than the wild type, showing weaker electrostatic and van der Waals interactions between the enzyme and the coenzyme or within the enzyme itself. The residue types at other positions were limited by similar considerations and analysis (data not shown). Significantly better coenzyme-dependency and thermostabilty were obtained by the electrostatic and van der Waals interactions between the enzyme and coenzyme, the same as the mutation at Tyr-64, as determined by the decomposed energy terms in the results of the MM calculations.

Fig. 2. Modeled Reductase S1 3-Dimensional Structure.
A complex structure of S1 reductase and NADPH created by homology modeling from the X-ray structures (see "Results") is shown as a ribbon diagram. The NADPH molecule is represented as CPK, and the eight residues to be mutated, position numbers 41–43, 47, and 63–66, are represented as ball-and-stick.

Table 1. Calculated Binding Energy to Coenzyme and Thermostability

mutated residues at position 64	binding energy $\Delta\Delta G_{bind}$ (kcal/mol)		thermostability $\Delta\Delta G$ (kcal/mol)
	NADH	NADPH	NADH complex
Ala	−21.3	39.7	−5.2
Arg	11.9	60.1	−6.4
Asn	−18.7	42.2	0.0
Asp	−11.1	66.0	−6.9
Cys	−8.9	18.5	−15.2
Gln	0.3	16.2	−22.7
Glu	−4.4	45.0	−9.2
Gly	7.6	39.9	−4.4
His	15.4	41.7	13.7
Ile	3.8	45.3	20.9
Leu	−17.0	58.2	15.5
Lys	−3.4	36.6	11.6
Met	−15.5	44.6	−4.6
Phe	7.3	41.9	−3.0
Pro	−6.3	48.4	25.6
Ser	0.4	45.9	−6.7
Thr	−5.3	17.8	−30.4
Trp	−1.5	74.0	12.8
Tyr (wt)	0.0	0.0	0.0
Val	−12.4	46.4	1.6

The results of the mutation at residue position 64 of reductase S1 are shown. The negative $\Delta\Delta G_{bind}$ and $\Delta\Delta G$ of the mutants mean better binding affinity and thermostability *versus* the wild type respectively.

Next, multiple-point mutations were calculated for these same residue positions to identify the desirable (*i.e.*, better affinity to NADH) single-point mutations. The residue positions in the multiple-point mutations were the same as those of the single-point mutations, and the residue types were selected and limited to particular types according to the results of the single-point mutations as: Ser-41 to Ala, Ser-42 to Ala or Arg, Ser-43 to Gly, Gln, or Arg, Tyr-47 to Arg, Trp-63 to Ile, Tyr-64 to Asp, Asn-65 to Ile or Val, and Ser-66 to Leu or Asn respectively, including their wild type residues. A total of 1,152 mutated sequences and their 3D structures were generated in the Shrike program. Of these, 144 mutants showed worse thermostabilty in the NADH holo-form than the wild type ($\Delta\Delta G > 100.0$ kcal/mol). This destabilization was caused primarily by the unfavorable van der Waals contacts of the mutated residues. The remaining 1,008 mutants were extracted and analyzed as candidates.

A summary of the calculated results is shown in Fig. 3 as scatter diagrams. Of the 1,008 generated mutants, 807 with possibly better NADH affinity and worse NADPH affinity were obtained disregarding their thermostability, according to the calculated coenzyme-binding energy (Fig. 3a). Meanwhile, many calculated mutants showed worse thermostability in NADH-bound holo-forms (Fig. 3b), and the mutants of only 306 sequences showed better thermostability than the wild type sequence disregarding their coenzyme specificity. Consequently, the mutants of 277 sequences showed both better NADH-dependency and better thermostability versus the wild type enzyme. The S1 mutants of 8 sequences (S1Mx) were finally selected from these 277 according to the orders of coenzyme specificity and thermostability. Their mutated residues are shown in Table 2. Essentially, mutations to Ser-41, Ser-42, Ser-43, Trp-63, Tyr-64, and Asn-65 appear to give NADH-dependency, and mutations to Tyr-47 and Ser-66 appear to give thermostability in the NADH-bound holo-form, considering the calculated results.

Expression and analysis of site-directed mutants

The selected S1 mutants were obtained by site-directed mutagenesis to the wild type S1. The resulting activities of these mutated enzymes, not purified but as a cell-free extraction, are shown in Table 2. All the designed mutants showed NADH dependency and lost their ability to utilize NADPH as a coenzyme. The ability to catalyze the asymmetric reduction of COBE was also retained in these eight S1 mutants, which gave (*S*)-CHBE with an optical purity of >99% e.e. These catalytic activities, however, were weaker than those of the wild type enzyme.

Among the mutants obtained, the S1M4 mutant showed better activity than others, so it was purified and its enzymatic properties were determined. Meanwhile, the S1M1 mutant was also purified because it was considered that the Arg-43 residue of S1M4 might cause or retain the NADPH-dependency of the mutant, according to the empirical analysis and comparison of the 1D structures (see Fig. 1), and the effect of the residue position of 43 was to be examined. The kinetic

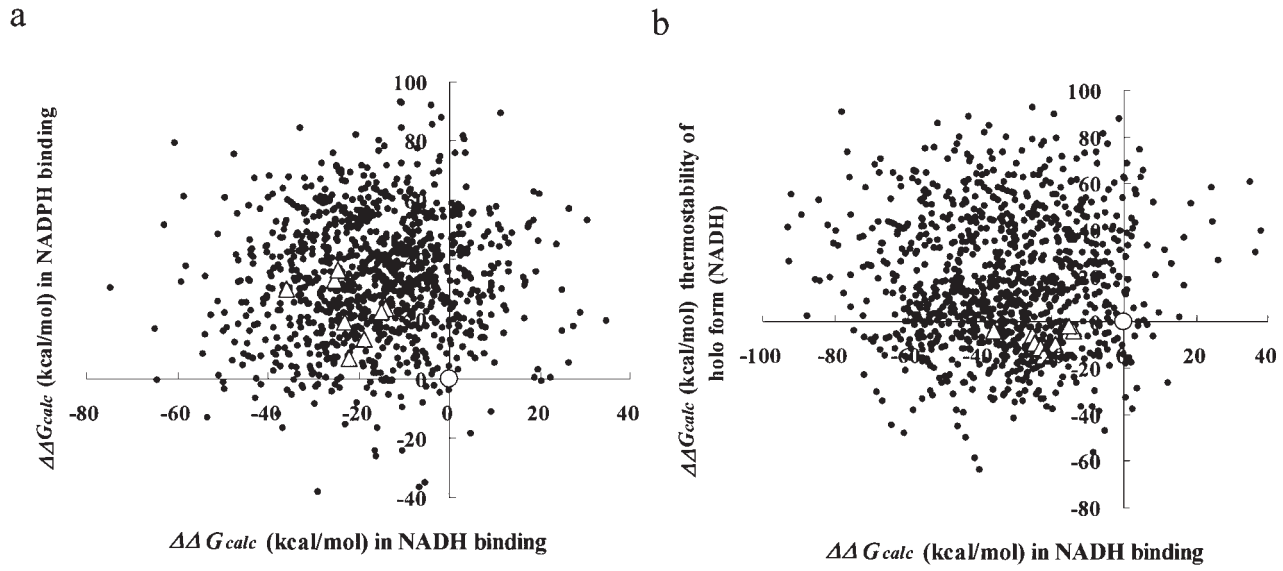

Fig. 3. Calculated Properties of Reductase S1 Mutants.

The results of the 8-point mutations are shown as a scatter diagram. Each virtual mutant is plotted as a small dot, the wild type (template) S1 as a big circle, and the 8 mutants (S1M1 to S1M8) as big triangles respectively. (a) The binding affinity of mutants to NADPH and NADH *vs.* the wild type is shown. The negative $\Delta\Delta G_{calc}$ of the mutants means better coenzyme affinity *versus* the wild type. Mutants plotted further to the left and higher in this diagram are expected to be NADH specific regardless of their thermostability and chemical stability. (b) The thermostability of the holo form (NADH) and the binding affinity of mutants to NADH *vs.* the wild type is shown. The negative $\Delta\Delta G_{calc}$ of the thermostability means better stability *versus* the wild type. Mutants plotted further to the left and lower in this diagram are expected to be thermostable and better NADH binding regardless of their NADPH affinity.

Table 2. Calculated and Experimental Properties of Reductase S1 Mutants

Enzyme	mutated residues	calculated binding energy $\Delta\Delta G_{bind}$ (kcal/mol)		calculated thermostability $\Delta\Delta G$ (kcal/mol)	experimental activity for COBE (U/ml)
	41–43/47/63–66	NADH	NADPH	NADH complex	/coenzyme
S1 (wt)	SSS/Y/WYNS	0.0	0.0	0.0	6.35/NADPH
S1M1	AAQ/Y/IDIN	−18.9	13.2	−9.9	1.11/NADH
S1M2	AAQ/Y/IDVL	−14.1	23.5	−3.6	0.37/NADH
S1M3	AAG/Y/IDIL	−25.3	33.1	−5.7	1.17/NADH
S1M4	AAR/Y/IDIN	−36.1	30.2	−4.0	3.02/NADH
S1M5	AAQ/R/IDIN	−24.7	36.9	−9.1	0.37/NADH
S1M6	AAR/R/IDIN	−23.1	18.9	−9.3	1.17/NADH
S1M7	ARS/Y/IDIN	−22.1	6.9	−14.7	0.51/NADH
S1M8	ARS/R/IDIN	−15.2	22.4	−2.0	0.08/NADH

The results for the experimentally obtained reductase S1 mutants are shown. The calculated negative $\Delta\Delta G_{bind}$ and $\Delta\Delta G$ of the mutants mean better binding affinity and thermostability versus the wild type, respectively. The experimental activity was determined with crude enzyme extracted solution.

Table 3. Kinetic Parameters of Wild Type and Designed Reductase S1 Mutants

Enzyme	activity for COBE (U/mg) /coenzyme	K_m for coenzyme (μM)		K_m for COBE (μM)	k_{cat} for coenzyme (sec^{-1})
		NADPH	NADH		
S1 (wt)	27.8/NADPH	16.7	N.D.	3.0	870 (NADPH)
S1M1	2.8/NADH	N.D.	160	3.9	64 (NADH)
S1M4	9.9/NADH	N.D.	62	2.6	120 (NADH)

The K_m and the k_{cat} for the coenzyme were determined under the condition of 10 mM COBE as a reactant, and N.D. in the K_m column means that the catalytic activity is not detected with each coenzyme. The K_m for COBE was determined under the condition of 5 mM coenzyme.

parameters of S1M1, S1M4, and the wild type S1 are shown in Table 3. The coenzyme-dependency of these mutants was inverted (see K_m for coenzyme), and their binding-affinity for the substrate was retained (see K_m for COBE), although the catalytic activity was slightly weakened (see k_{cat} for coenzyme). The thermostability of the mutants was not changed versus the wild type. After heat treatment, they retained their catalytic activity

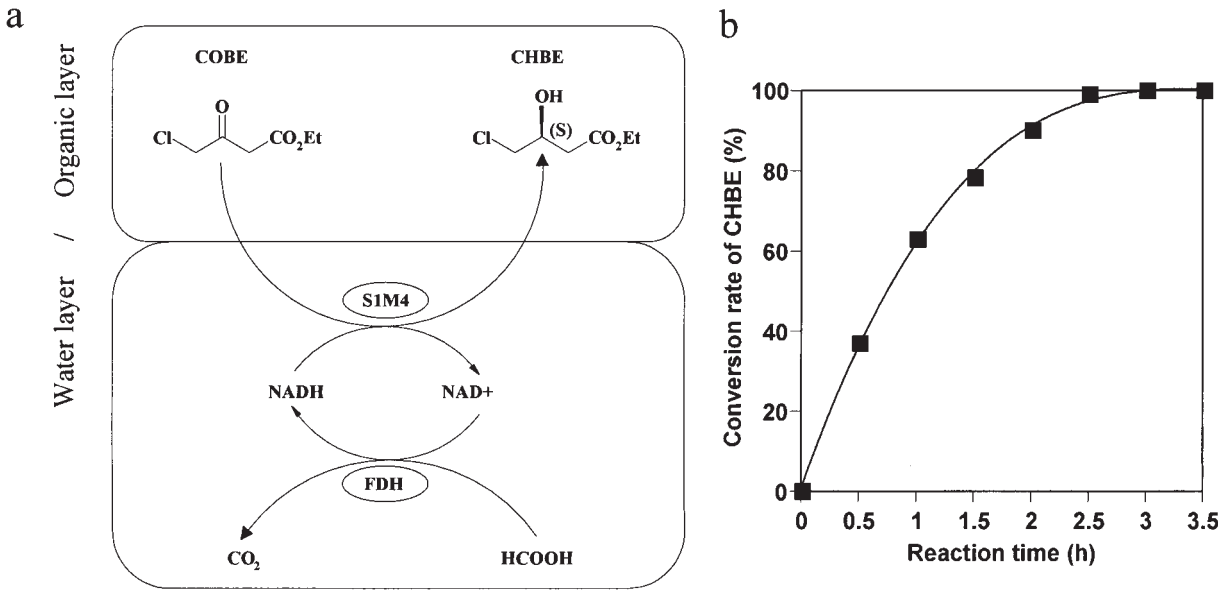

Fig. 4. Synthesis of (S)-CHBE by Mutated S1 (S1M4).

(a) The reaction scheme of a water–organic two-phase asymmetric reduction system cooperating with the coenzyme regeneration system is shown. The reactant COBE and the product CHBE are in an organic layer, and the enzymes (S1M4, FDH), coenzyme NADH, and formate are in a water layer. (b) The reaction profile as the conversion rate of the product CHBE from COBE is shown.

up to 45 °C and then lost it at temperatures over 50 °C (data not shown).

Reduction of COBE with S1M4 and formate dehydrogenase (FDH) in a two-phase system

The results of the asymmetric reduction of COBE by S1M4 reductase and NADH in an organic/water two-phase system in cooperation with the NADH regenerating system of FDH and formate are shown in Fig. 4. The catalytic reduction of COBE (162 g/l) with S1M4 gave CHBE (163 g/l), and the turnover rate of NAD+ based on the amounts of NAD+ added and CHBE formed was approximately 1,000 mol/mol. The conversion rate from COBE to CHBE was >99% after 3.5 h (Fig. 4b), and the optical purity of the resulting alcohol was >99% e.e. In this two-phase system, S1M4 showed good tolerance to the organic solvent as well as the wild type S1.

Discussion

The conserved residues GXXXGXG are known as the nicotinamide-coenzyme binding motif in the SDR family,[3] and S1 has the same motif (Gly-40, Gly-44, and Gly-46). In NADPH-dependent SDRs (Fig. 1b), Arg or Lys that bind to adenosine 2′-phosphate of NADPH with an electrostatic interaction, are almost always conserved, but S1 has different residues at the corresponding residue positions (Ser-43, Tyr-47, and Asn-65). Several NADH-dependent SDRs also have Arg or Lys at these positions, so these cationic residues might be preferable for, but not critical to, NADPH-dependency. Meanwhile, in NADH-dependent SDRs (Fig. 1a), Asp, which binds to adenosine 2′,3′-diol of NADH, is almost always conserved, but S1 has a different residue at that residue position (Tyr-64). Asp at this position might be critical to NADH-dependency because the carboxylate of the Asp side-chain can form a "bi-dental" strong electrostatic nonbonded interaction to adenosine 2′,3′-diol of NADH. In comparison, the anionic side-chain of Asp repulses the adenosine 2′-phosphate anion of NADPH. S1 does not have these features in its amino acid sequence, which would confer distinct NADPH- or NADH-dependency. It is not clear how the S1 enzyme distinguishes between NADPH and NADH based on analysis of its 1D structure, but, according to our comparisons with the 1D structures of SDRs, a mutation of Tyr-64-Asp onto S1 is considered to be the best choice to invert the coenzyme-dependency of S1. On the other hand, the mutation of Thr-38-Asp onto mouse lung carbonyl reductase (CR), another member of the SDR family, was studied by Nakanishi *et al.*,[12] and that mutant showed NADH-dependency. Thr-38 in mouse lung CR occupies the same position as Tyr-64 in S1 in the 3D structure, so the mutation Tyr-64-Asp onto S1 is also expected to invert the coenzyme specificity.

The correlation between the difference in the calculated NADH-binding energy $\Delta\Delta G_{bind}$ and the experimental activity of the S1 mutants was found to be semi-quantitative (its correlation coefficient $R = 0.88$) with the regression analysis (Table 2). Hence it was assumed that the regained NADH-binding energy ΔG_{bind}, which is equivalent to the binding constant (dissociation constant) K_m of the enzyme for NADH (eq. 1), made a significant contribution to the NADH-dependency to those S1 mutants. Meanwhile, it was difficult to analyze the individual influences of those mutated residues on the properties of the S1 mutants, as these multiple-point mutations were introduced to the residues adjacent to

Table 4. Calculated Binding Energy to Coenzyme and Thermostability

residue wild-type	residue mutated	calculated binding energy $\Delta\Delta G_{bind}$ (kcal/mol) NADH	calculated binding energy $\Delta\Delta G_{bind}$ (kcal/mol) NADPH	calculated thermostability $\Delta\Delta G$ (kcal/mol) NADH complex
Ser-41	Ala	−22.9	16.4	−8.8
Ser-42	Ala	−11.9	52.9	−13.6
	Arg	−3.4	82.2	−4.5
Ser-43	Gln	19.9	33.1	16.4
	Gly	2.8	52.2	25.4
	Arg	0.8	35.7	16.3
Tyr-47	Arg	20.7	52.4	−10.9
Trp-63	Ile	−12.1	58.2	9.0
Tyr-64	Asp	−11.1	66.0	−6.9
Asn-65	Ile	−4.4	44.2	14.1
	Val	−13.8	39.0	13.1
Ser-66	Asn	7.0	18.0	−5.2
	Leu	10.8	34.1	−7.2

The results of the one-point mutation at residue positions 41, 42, 43, 47, 63, 64, 65, and 66 of reductase S1 (see also Table 2) are shown. The negative $\Delta\Delta G_{bind}$ and $\Delta\Delta G$ of the mutants means better binding affinity and thermostability versus the wild type, respectively.

each other. As such, the simple energy-decomposition analysis gave unclear and complicated results (data not shown). The individual effects of each mutated residue in the S1 mutants were estimated with the results of calculated single-point mutations at those residues. The summarized results are shown in Table 4.

The common mutations of Ser-41-Ala, Trp-63-Ile, and Tyr-64-Asp to S1Mx were estimated to give better NADH-dependency, and those mutants were estimated to give lower nonbonded interaction energies (electrostatic, van der Waals, and solvation energy terms) based on the energy-decomposition analysis. The shape of their coenzyme-binding pocket might therefore be fitted to an NADH molecule, and it was considered that these mutations might result in substantial effects on the inverted coenzyme specificity. The mutation of Tyr-47-Arg was estimated to give better thermostability but worse NADH-dependency. As a result, S1M5, S1M6, and S1M8 showed weaker activity with NADH as a coenzyme than did S1M1, S1M4, and S1M7 respectively. Both mutations of Ser-42-Ala and of Ser-42-Arg were estimated to give better NADH-dependency and thermostability. The former, however, was more effective in its enzymatic properties than the latter, so that S1M7 and S1M8 might show weaker activity for COBE than the other S1Mx. The mutations of Ser-43-Gln, Ser-43-Gly, and Ser-43-Arg were estimated to give somewhat worse NADH affinity under the condition of the single-point mutation, but they were estimated to give even worse NADPH affinity, which might affect the NADH-specificity. The mutation of Ser-43-Arg was estimated to give rather better NADH affinity than Ser-43-Gln, so that S1M4 might show better activity than S1M1, although the analysis of the 1D structures of the SDRs showed that the mutation of Ser-43-Arg appeared to be preferable to NADPH-dependency (Fig. 1b). The mutation of Asn-65-Val was estimated to give better NADH-dependency than Asn-65-Ile under the condition of the single-point mutation, but the calculated enzymatic properties of S1M2 (Asn-65-Val) and S1M1 (Asn-65-Ile) were inverted in the multiple-point mutation (Table 2), so that S1M2 might show worse specific activity than S1M1. The mutations of Ser-66-Asn and Ser-66-Leu were estimated to give poor coenzyme specificity but slightly better thermostability, and those effects were unclear in the multiple-point mutants but might have resulted in slightly better thermostability in the holo-form S1Mx. Consequently, the effects of each of the single-point mutations must accumulate and balance one another more effectively in the amino acid sequence of S1M4 than in the other S1Mx.

The mutated residue positions were at a distance from the substrate-binding pocket of S1Mx, so it was difficult to explain their weakened catalytic activity. The k_{cat} and V_{max} values of the enzyme for a substrate such as COBE could not be estimated by the design method reported here. These mutations might cause some perturbation of the substrate-binding pocket of the mutated reductases *versus* the wild type. As a result, the orientation and distance between the nicotinamide moiety of the coenzyme and the spatial configuration of the substrate molecule for the enzyme would become unsuitable to the catalytic reduction, possibly resulting in weaker activity. However, the results of the CHBE synthesis from COBE (Fig. 4b) showed that S1M4 has high catalytic activity and availability to use the NADH coenzyme and is applicable to the asymmetric reduction of ketones with the NADH coenzyme, as intended. The rational design method in this work must be applicable to exchanging the coenzyme specificity or substrate specificity of other enzymes.

References

1) Wada, M., Kataoka, M., Kawabata, H., Yasohara, Y., Kizaki, N., Hasegawa, J., and Shimizu, S., Purification and characterization of NADPH-dependent carbonyl reductase, involved in stereoselective reduction of ethyl 4-chloro-3-oxobutanoate, from *Candida magnoliae*. *Biosci. Biotechnol. Biochem.*, **62**, 280–285 (1998).
2) Yasohohara, Y., Kizaki, N., Hasegawa, J., Wada, M., Kataoka, M., and Shimizu, S., Molecular cloning and overexpression of the gene encoding an NADPH-dependent carbonyl reductase from *Candida magnoliae*, involved in stereoselective reduction of ethyl 4-chloro-3-oxobutanoate. *Biosci. Biotechnol. Biochem.*, **64**, 1430–1436 (2000).
3) Persson, B., Krook, M., and Joernvall, H., Characteristics of short-chain alcohol dehydrogenases and related enzymes. *Eur. J. Biochem.*, **200**, 537–543 (1991).
4) Kizaki, N., Yasohara, Y., Hasegawa, J., Wada, M., Kataoka, M., and Shimizu, S., Synthesis of optically pure ethyl (*S*)-4-chloro-3-hydroxybutanoate by *Escherichia coli* transformant cells coexpressing the carbonyl reductase and glucose dehydrogenase genes. *Appl. Microbiol. Biotechnol.*, **55**, 590–595 (2001).

5) Kataoka, M., Kita, K., Wada, M., Yasohara, Y., Hasegawa, J., and Shimizu, S., Novel bioreduction system for the production of chiral alcohols. *Appl. Microbiol. Biotechnol.*, **62**, 437–445 (2003).
6) Nanba, H., Takaoka, Y., and Hasegawa, J., Purification and characterization of formate dehydrogenase from *Ancylobacter aquaticus* strain KNK607M, and cloning of the gene. *Biosci. Biotechnol. Biochem.*, **67**, 720–728 (2003).
7) Scrutton, N. S., Berry, A., and Perham, N., Redesign of the coenzyme specificity of a dehydrogenase by protein engineering. *Nature*, **343**, 38–43 (1990).
8) Bocanegra, J. A., Scrutton, N. S., and Perhama, R. N., Creation of an NADP-dependent pyruvate dehydrogenase multienzyme complex by protein engineering. *Biochemistry*, **32**, 2737–2740 (1993).
9) Chen, R., Greer, A., and Dean, A. M., A highly active decarboxylating dehydrogenase with rationally inverted coenzyme specificity. *Proc. Natl. Acad. Sci. U.S.A.*, **92**, 11666–11670 (1995).
10) Holmberg, N., Ryde, U., and Buelow, L., Redesign of the coenzyme specificity in L-lactate dehydrogenase from *Bacillus stearothermophilus* using site-directed mutagenesis and media engineering. *Protein Engineering*, **12**, 851–856 (1999).
11) Galkin, A., Kulakova, L., Ohshima, T., Esaki, N., and Soda, K., Construction of a new leucine dehydrogenase with preferred specificity for NADP+ by site-directed mutagenesis of the strictly NAD+ specific enzyme. *Protein Engineering*, **10**, 687–690 (1997).
12) Nakanishi, M., Matsuura, K., Kaibe, H., Tanaka, N., Nonaka, T., Mitsui, Y., and Hara, A., Switch of coenzyme specificity of mouse lung carbonyl reductase by substitution of threonine 38 with aspartic acid. *J. Biol. Chem.*, **272**, 2218–2222 (1997).
13) Morikawa, S., and Nakai, T., Japan Kokai Tokkyo Koho, 2001-184381 (July 6, 2001).
14) Desmet, J., De Maeyer, M., Hazes, B., and Lasters, I., The dead-end elimination theorem and its use in protein side-chain positioning. *Nature*, **356**, 539–542 (1992).
15) Weiner, S. J., Kollman, P. A., Nguyen, D. T., and Case, D. A., An all atom force field for simulation for proteins and nucleic acids. *J. Comput. Chem.*, **7**, 230–252 (1986).
16) Stouten, P. F. W., Froemmel, C., Nakamura, H., and Sander, C., An effective solvation term based on atomic occupancies for use in protein simulations. *Mol. Simulation*, **10**, 97–120 (1993).
17) D'Aquino, J., Gomez, J., Hilser, V. J., Lee, K. H., and Amzel, L. M., Magnitude of the backbone conformational entropy change in protein folding. *Proteins*, **25**, 143–156 (1996).
18) Doig, A. J., and Sternberg, M. J. E., Side chain conformational entropy in protein. *Protein Science*, **4**, 2247–2251 (1995).
19) Altschul, S. F., Gish, W., Miller, W., Myers, E. W., and Lipman, D. J., Basic local alignment search tool. *J. Mol. Biol.*, **215**, 403–410 (1990).
20) Thompson, J. D., Gibson, T. J., Plewniak, F., Jeanmougin, F., and Higgins, D. G., The ClustalX windows interface: Flexible strategies for multiple sequence alignment aided by quality analysis tools. *Nucleic Acids Res.*, **24**, 4876–4882 (1997).
21) Guex, N., and Peitsch, M. C., SWISS-MODEL and the Swiss-PDB Viewer: An environment for comparative protein modeling. *Electrophoresis*, **18**, 2714–2723 (1997).
22) Nanba, H., Takaoka, Y., and Hasegawa, J., Purification and characterization of an α-haloketone-resistant formate dehydrogenase from *Thiobacillus* sp. strain KNK65MA, and cloning of the gene. *Biosci. Biotechnol. Biochem.*, **67**, 2145–2153 (2003).
23) Yasohara, Y., Kizaki, N., Hasegawa, J., Takahashi, S., Wada, M., Kataoka, M., and Shimizu, S., Synthesis of optically active ethyl 4-chloro-3-hydroxybutanoate by microbial reduction. *Appl. Microbiol. Biotechnol.*, **51**, 847–851 (1999).